

Observation of the bottomonium ground state, η_b , at BaBar

P. Grenier

SLAC, 2575 Sand Hill Road, Menlo Park, CA 94025, USA and

Representing the BaBar Collaboration

We present the first observation of the bottomonium ground state $\eta_b(1S)$ in the photon energy spectrum using a sample of (109 ± 1) million of $\Upsilon(3S)$ events recorded at the $\Upsilon(3S)$ energy with the BaBar detector at the PEP-II B factory at SLAC. A peak at $E_\gamma = 921.2_{-2.8}^{+2.1}(\text{stat}) \pm 2.4(\text{syst})$ MeV observed with a significance of 10 standard deviations in the photon energy spectrum is interpreted as being due to the radiative transition $\Upsilon(3S) \rightarrow \gamma \eta_b(1S)$. This photon energy corresponds to an $\eta_b(1S)$ mass of $9388.9_{-2.3}^{+3.1}(\text{stat}) \pm 2.7(\text{syst})$ MeV/ c^2 . The hyperfine $\Upsilon(1S)$ - $\eta_b(1S)$ mass splitting is $71.4_{-3.1}^{+2.3}(\text{stat}) \pm 2.7(\text{syst})$ MeV/ c^2 . The branching fraction for this radiative $\Upsilon(3S)$ decay is obtained as $(4.8 \pm 0.5(\text{stat}) \pm 1.2(\text{syst})) \times 10^{-4}$.

1. INTRODUCTION

Bottomonium spectroscopy started thirty years ago with the discovery of the $\Upsilon(nS)$ resonances [1]. The spin-singlet states $h_b(nP)$ and $\eta_b(nS)$ have yet to be observed. In particular, the ground state of the bottomonium spectrum, $\eta_b(1S)$, was still missing. The mass difference between the $\Upsilon(1S)$ and the $\eta_b(1S)$, the hyperfine splitting, is very important in understanding the role of spin-spin interaction in heavy quark bound systems and in testing calculations and predictions from various models such as Quark Models, pNRCQCD and Lattice QCD [2]. Predictions for the hyperfine splitting vary from 36 to 100 MeV/ c^2 [3].

We report on the observation of the bottomonium ground state η_b from the radiative transition $\Upsilon(3S) \rightarrow \gamma \eta_b$ [4]. Theoretical predictions for the branching fraction of the decay vary from 1 to 20×10^{-4} [3]. The CLEO III experiment has published a 90% confidence level upper limit for the branching fraction $\mathcal{B}[\Upsilon(3S) \rightarrow \gamma \eta_b] < 4.3 \times 10^{-4}$ [5].

The data used in this study was recorded with the BaBar detector [6] at the PEP-II asymmetric-energy e^+e^- storage rings. It consists of 28.0 fb^{-1} of integrated luminosity collected at a e^+e^- CM energy of 10.355 GeV, corresponding to the mass of the $\Upsilon(3S)$ resonance. Samples of 2.4 fb^{-1} and 43.9 fb^{-1} recorded 30 MeV below the $\Upsilon(3S)$ and 40 MeV below the $\Upsilon(4S)$ resonances were used for background studies. The trajectories of charged particles are reconstructed using a combination of five layers of double-sided silicon strip detectors and a 40-layer drift chamber, all operated inside the 1.5-T magnetic field of a superconducting solenoid. Photons are detected using a CsI(Tl) electromagnetic calorimeter (EMC), which is also inside the coil. The energy resolution for photons varies from 2.9% (at 600 MeV) to 2.5% (at 1400 MeV).

2. BACKGROUNDS AND SIGNAL SELECTION

The signal for $\Upsilon(3S) \rightarrow \gamma \eta_b$ is extracted from a binned maximum likelihood fit to the inclusive photon energy spectrum in the center of mass (CM) frame. The monochromatic photon from the decay will appear as a bump in the photon energy (E_γ) distribution. For an η_b mass of 9.4 GeV, and the $\Upsilon(3S)$ energy, the photon energy shall peak at 911 MeV. We are therefore looking for an enhancement in the E_γ distribution near 900 MeV.

2.1. Background contributions to the E_γ distribution

There are two main background contributions to the photon energy distribution. The first contribution produces a smooth non-peaking background. It comes from continuum events ($e^+e^- \rightarrow q\bar{q}$ where $q = u, d, s, c$) and bottomonium decays. The second contribution produces peaks in the E_γ spectrum, close to the expected signal position. It comes from two processes:

- The exclusive decay $\Upsilon(3S) \rightarrow \gamma\chi_{bJ}(2P); \chi_{bJ}(2P) \rightarrow \gamma\Upsilon(1S)$, $J = 0, 1, 2$. The second radiative transitions produce a broad peak centered at 760 MeV. As there are three transitions, we would expect to observe three peaks. However, due to the detector energy resolution and to the Doppler broadening, that arises from the motion of the $\chi_{bJ}(2P)$ states in the $\Upsilon(3S)$ CM frame, the three peaks merge into a single broad bump.
- The radiative production of the $\Upsilon(1S)$ through initial state radiation (ISR): $e^+e^- \rightarrow \gamma_{ISR}\Upsilon(1S)$. This process produces a peak centered at 856 MeV.

In order to extract the η_b signal, it is crucial to understand both the lineshapes and the yields of the two peaking background components.

2.2. Signal Selection

The selection criteria have been optimized by maximizing the figure of merit S/\sqrt{B} , where S and B represent the expected yield for signal and background respectively. The signal sample is obtained from a detailed Monte Carlo (MC) simulation. There is no reliable event generator to model the various bottomonium decays. A small fraction (9%) of the data sample (in the region $0.85 < E_\gamma < 0.95$ GeV) was used to model the background. In order to avoid any bias, this small data set was not used for the extraction of the signal in the final fit.

As the η_b is expected to decay mainly through two gluons, one can expect a large track multiplicity in the final state. Events are selected by requiring at least four tracks in the event and that the ratio of the second to zeroth Fox-Wolfram moments [7] be less than 0.98.

Photons are first required to be isolated from all charged tracks, and their shapes are required to be consistent with an electromagnetic shower: the lateral moments [8] are required to be less than 0.55. In order to reduce the contribution from ISR events $e^+e^- \rightarrow \gamma_{ISR}\Upsilon(1S)$, candidate photons are required to be detected in the central region of the calorimeter $-0.762 < \cos(\theta_{\gamma,LAB}) < 0.890$, where $\theta_{\gamma,LAB}$ is the angle between the photon and the beam axis in the laboratory frame.

We apply a cut on the angle θ_T between the direction of the photon momentum and the thrust axis [9]. The thrust axis is computed with all charged tracks and neutral calorimeter clusters in the event, excluding the photon candidate. Given that the η_b is a spin-zero resonance, the angle distribution for the signal should be flat. However, for continuum events the distribution should be peaking at the forward and backward directions. We require $|\cos\theta_T| < 0.7$.

Finally we apply a veto to reduce photons coming from π^0 decays. These photons represents the main source of background. A photon candidate combined with any photons in the event is required not to have an invariant mass within 15 MeV of the nominal π^0 mass. The energy of the second photon in the π^0 candidate is required to be larger than 50 MeV.

These selection criteria lead to an efficiency of 37% and 6% on signal and background respectively.

The optimization procedure was checked on data using the broad peak from the second radiative transition of the $\Upsilon(3S) \rightarrow \gamma\chi_{bJ}(2P); \chi_{bJ}(2P) \rightarrow \gamma\Upsilon(1S)$ process. It yielded to a very similar cut optimization.

3. FITTING PROCEDURE

3.1. Introduction

The η_b signal is extracted, after all selection cuts are applied, using a binned maximum likelihood fit to the inclusive photon energy spectrum in the CM frame in the range $0.5 < E_\gamma < 1.1$ GeV.

There are four components to the fit:

- non-peaking background;
- $\chi_{bJ}(2P) \rightarrow \gamma\Upsilon(1S)$ peaking background;

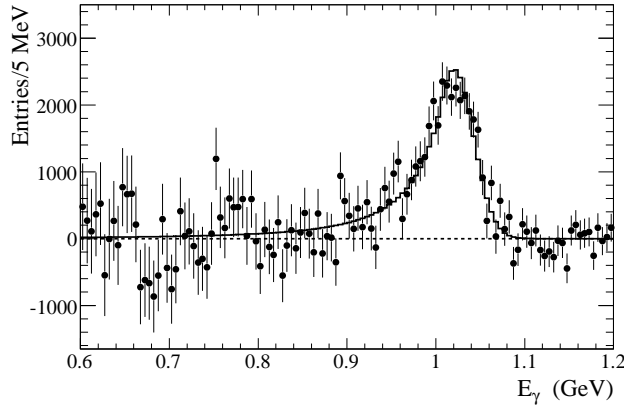
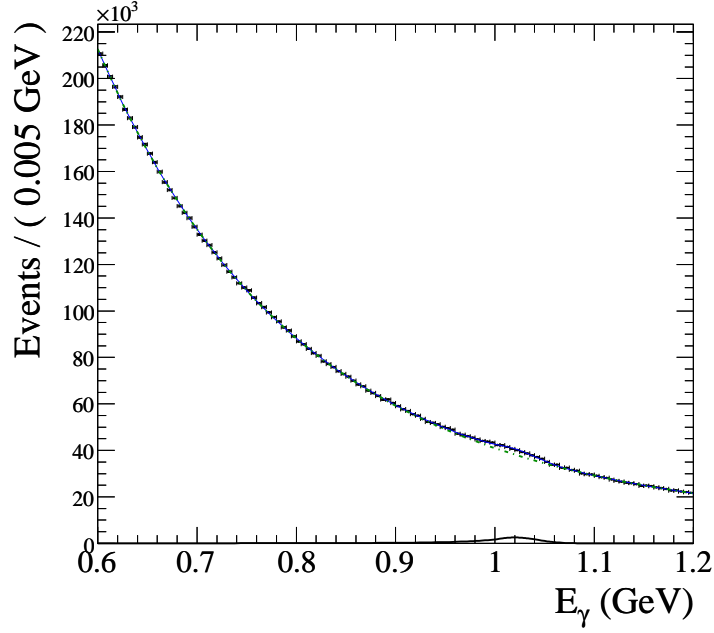


Figure 1: The top figure shows the E_γ distribution from the $\Upsilon(4S)$ Off-Peak data sample. The bottom figure shows the background subtracted distribution. The $\gamma_{ISR}\Upsilon(1S)$ peak is clearly visible.

- $\gamma_{ISR}\Upsilon(1S)$ peaking background;
- η_b signal.

3.2. Probability density functions

The non-peaking background has been parametrized by the following probability density function: $f(E_\gamma) = A (C + \exp[-\alpha E_\gamma - \beta E_\gamma^2])$.

As explained above, due to detector energy resolution and Doppler broadening, the three peaks from the $\chi_{bJ}(2P) \rightarrow \gamma \Upsilon(1S)$ transitions are merged. The three peaks have been modeled using a Gaussian modified with a power-law tail on the low side (Crystall Ball (CB) function [10]). The relative rates and peak positions between the three peaks have been fixed from the PDG values [11]. For each $\chi_{bJ}(2P)$ lineshape, the parameters of the power-law tail have been fixed to a common value. The PDF parameters have been determined from fitting non-peaking background subtracted the E_γ distribution where the signal region (840 to 960 MeV) has been excluded (see Figure 2). For the

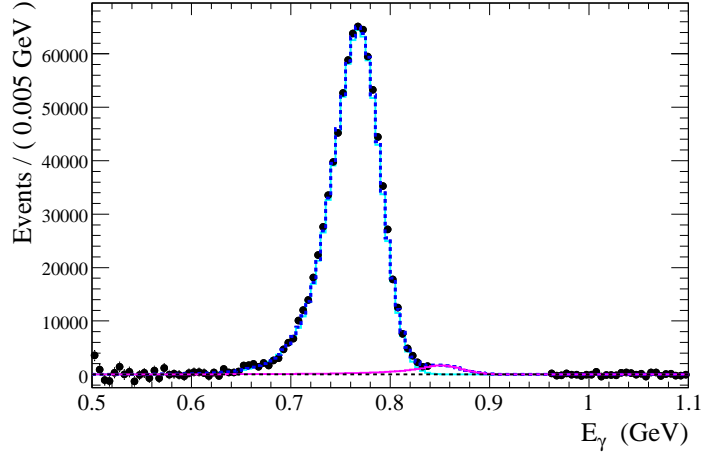


Figure 2: Fit to the background subtracted E_γ distribution, with the signal excluded, for the determination of the $\chi_{bJ}(2P) \rightarrow \gamma \Upsilon(1S)$ PDF parameters. The blue dotted line shows the $\chi_{bJ}(2P) \rightarrow \gamma \Upsilon(1S)$ lineshape and the full purple line shows the $\gamma_{ISR} \Upsilon(1S)$ lineshape.

final fit, all the $\chi_{bJ}(2P) \rightarrow \gamma \Upsilon(1S)$ component parameters were fixed to the values obtained from this fit, except the yield.

The PDF for the $\gamma_{ISR} \Upsilon(1S)$ (i.e. ISR peak) peaking background component was modeled with a CB function. All the CB parameters were obtained from MC. Given the detector energy resolution, the ISR and signal peaks are likely to overlap. Depending on the mass of the η_b , the overlap could be large. In the final fit, it was therefore decided to fix the yield of the ISR peak. The rate of the ISR peak was estimated using data taken 40 MeV below the $\Upsilon(4S)$ resonance ($\Upsilon(4S)$ Off-Peak data). The top plot of Figure 1 shows the E_γ distribution for the $\Upsilon(4S)$ Off-Peak data after all cuts are applied. The bottom plot shows the same distribution after subtracting the non-peaking background. A clear ISR peak is seen. A fit with a CB functions yields to 35800 ± 1600 events. The yield is extrapolated to the $\Upsilon(3S)$ energy using the relative cross-sections, integrated luminosities and signal reconstruction efficiencies. The estimated $\gamma_{ISR} \Upsilon(1S)$ yield is then 25200 ± 1700 events. The error includes systematic uncertainties. This is consistent with but more precise than the yield estimated with data taken below the $\Upsilon(3S)$ resonance.

The η_b PDF is modeled with a non-relativistic Breit-Wigner function (for the natural shape of the η_b) convolved with a CB function which models the energy resolution. The CB parameters were fixed from MC. MC experiments have shown that the width of the η_b had to be fixed in the final fit. It is not known, but theoretical prediction vary from 4 to 20 MeV [12]. We used a value of 10 MeV for the nominal fit.

3.3. Fit to the full data sample

The final fit to the E_γ distribution was performed with the PDFs described above. The free parameters were the $\chi_{bJ}(2P) \rightarrow \gamma \Upsilon(1S)$ process yield, the non-peaking background parameters and the signal yield. Figure 3(a) shows the E_γ distribution and the fit result. In addition to the non-peaking background, only the $\chi_{bJ}(2P) \rightarrow \gamma \Upsilon(1S)$ broad peak is visible. Figure 3(b) shows the non-peaking background subtracted plot in the signal region. The $\chi_{bJ}(2P) \rightarrow \gamma \Upsilon(1S)$, $\gamma_{ISR} \Upsilon(1S)$, and signal peaks are clearly visible. Figure 3(c) shows the background subtracted distribution overlaid with the fit result for the η_b PDF.

The fitted η_b signal yield is $19200 \pm 2000 \pm 2100$ events, where the first error is statistical and the second systematic. The systematic error has been obtained from varying the η_b width (from 5 to 20 MeV), the $\gamma_{ISR} \Upsilon(1S)$ yield within $\pm 1 \sigma$ of the nominal value, and the PDF parameters within $\pm 1 \sigma$.

The η_b signal significance is estimated using the ratio $\log(L_{\max}/L_0)$, where L_{\max} and L_0 are the likelihood values obtained from the nominal fit and from a fit with the η_b PDF removed, respectively. The significance the signal has

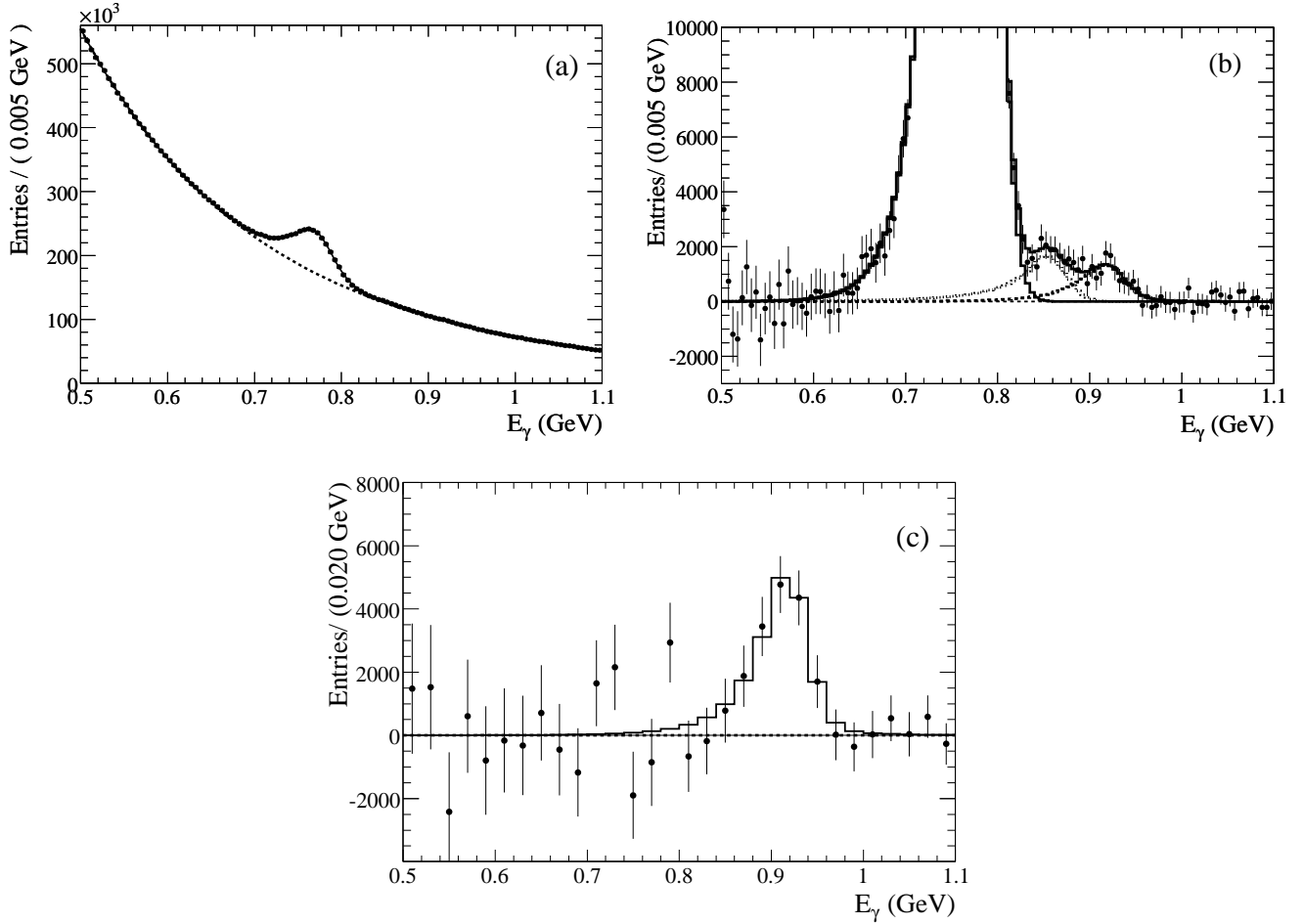


Figure 3: (a) Inclusive E_γ distribution with fit result. Only the $\chi_{bJ}(2P) \rightarrow \gamma \Upsilon(1S)$ is visible. (b) Non-peaking background subtracted plot, with PDFs for $\chi_{bJ}(2P) \rightarrow \gamma \Upsilon(1S)$ peak (solid), ISR peak (dot), η_b signal (dash) and the sum of all three (solid). (c) All-background subtracted distribution.

been conservatively estimated with the following method: a fit to the data has been performed with all parameters entering the systematic errors moved by 1 standard deviation in the direction of smallest significance. This method yields to a 10 standard deviations significance.

4. RESULTS

The fitted η_b signal position is $917.4^{+2.1}_{-2.8}$ MeV. A photon energy calibration shift of 3.8 ± 2.0 MeV is then applied. It is obtained by comparing the fitted position of the $\chi_{bJ}(2P) \rightarrow \gamma \Upsilon(1S)$ peak to the PDG value. Applying the energy calibration shift, we obtain for the peak position of the η_b signal: $E_\gamma = 921.2^{+2.1}_{-2.8} \pm 2.4$ MeV.

This yields to the η_b mass: $M(\eta_b) = 9388.9^{+3.1}_{-2.3} \pm 2.7$ MeV/ c^2 . Using the PDG value of 9460.3 ± 0.3 MeV/ c^2 for the $\Upsilon(1S)$ mass, we determine the $\Upsilon(1S)$ - η_b mass splitting to be $71.4^{+2.3}_{-3.1} \pm 2.7$ MeV/ c^2 .

Using the signal reconstruction efficiency and the number of $\Upsilon(3S)$ events, we estimate the $\Upsilon(3S) \rightarrow \gamma \eta_b$ branching fraction to be $(4.8 \pm 0.5 \pm 1.2) \times 10^{-4}$, where the first uncertainty is statistical and the second systematic. The main systematic uncertainty is from the efficiency. We have compared the reconstruction efficiency of the $\chi_{bJ}(2P) \rightarrow \gamma \Upsilon(1S)$ peak between data and MC, giving a 18% error.

5. CONCLUSION

In conclusion, we have made the first observation of the bottomonium ground state, the η_b . The new state has been observed in the radiative decay of the $\Upsilon(3S)$. The η_b is the most likely interpretation of the signal, although other hypothesis are not excluded. The mass of the η_b is $9388.9_{-2.3}^{+3.1} \pm 2.7$ MeV/ c^2 , which corresponds to a mass splitting between the $\Upsilon(1S)$ and the η_b of $71.4_{-3.1}^{+2.3} \pm 2.7$ MeV/ c^2 . The estimated branching fraction of the decay $\Upsilon(3S) \rightarrow \gamma \eta_b$ is found to be $(4.8 \pm 0.5 \pm 1.2) \times 10^{-4}$.

Acknowledgments

The author is representing the BaBar Collaboration. We are grateful for the excellent luminosity and machine conditions provided by our PEP-II colleagues, and for the substantial dedicated effort from the computing organizations that support BaBar. We thank Bob McElrath and Michael Peskin for helpful discussions. The collaborating institutions wish to thank SLAC for its support and kind hospitality. This work is supported by DOE and NSF (USA), NSERC (Canada), CEA and CNRS-IN2P3 (France), BMBF and DFG (Germany), INFN (Italy), FOM (The Netherlands), NFR (Norway), MES (Russia), MEC (Spain), and STFC (United Kingdom). Individuals have received support from the Marie Curie EIF (European Union) and the A. P. Sloan Foundation.

References

- [1] S.W. Herb et al., Phys. Rev. Lett. **39**, 252 (1977); W.R. Innes et al., Phys. Rev. Lett. **39**, 1240 (1977) [Erratum-ibid. **39**, 1640(E) (1977)].
- [2] For a comprehensive review, see N. Brambilla *et al.* [Quarkonium Working Group], CERN Yellow Report, CERN-2005-005 (2005).
- [3] S. Godfrey and J.L. Rosner, Phys. Rev. D **64**, 074011 (2001) [Erratum-ibid. **65**, 039901(E) (2002)], and references therein.
- [4] B. Aubert et al. [BABAR Collaboration], Phys. Rev. Lett. **101**, 071801 (2008).
- [5] M. Artuso et al. [CLEO III Collaboration], Phys. Rev. Lett. **94**, 032001 (2005).
- [6] B. Aubert et al. [BABAR Collaboration], Nucl. Instrum. Methods Phys. Res., Sect A **479**, 1 (2002).
- [7] G.C. Fox and S. Wolfram, Nucl. Phys. **B149**, 413 (1979).
- [8] A. Drescher et al. [ARGUS Collaboration], Nucl. Instrum. Methods Phys. Res., Sect A **237**, 464 (1985).
- [9] S. Brandt et al., Phys. Lett. **12**, 57 (1964); E. Fahri, Phys. Rev. Lett. **39**, 1587 (1977).
- [10] J.E. Gaiser, Appendix-F Charmonium Spectroscopy from Radiative Decays of the J/ψ and ψ' , Ph.D. thesis, SLAC-R-255 (1982).
- [11] W.-M. Yao et al. (Particle Data Group), J. Phys. G **33**, 1 (2006) and 2007 partial update for the 2008 edition.
- [12] W. Kwong et al., Phys. Rev. D **37**, 3210 (1988); C.S. Kim, T. Lee, and G.L. Wang, Phys. Lett. **B606**, 323 (2005). J.P. Lansberg and T.N. Pham, Phys. Rev. D **75**, 017501 (2007).